

**An investigation into the use of polymer blends to improve the printability of and regulate drug release from pharmaceutical solid dispersions prepared via fused deposition modeling (FDM) 3D printing**

Muqdad Alhijaj<sup>1,2</sup>, Peter Belton<sup>3</sup>, and Sheng Qi<sup>1\*</sup>

- 
1. *School of Pharmacy, University of East Anglia, Norwich, Norfolk, UK, NR4 7TJ*
  2. *Department of Pharmaceutics, College of Pharmacy, University of Basrah, Basrah, Iraq*
  3. *School of Chemistry, University of East Anglia, Norwich, Norfolk, UK, NR4 7TJ*

Correspondence: Sheng Qi, [sheng.qi@uea.ac.uk](mailto:sheng.qi@uea.ac.uk); Fax number: +44 1603592023

## **Abstract**

FDM 3D printing has been recently attracted increasing research efforts towards the production of personalized solid oral formulations. However, commercially available FDM printers are extremely limited with regards to the materials that can be processed to few types of thermoplastic polymers, which often may not be pharmaceutically approved materials nor ideal for optimizing dosage form performance of poor soluble compounds. This study explored the use of polymer blends as a formulation strategy to overcome this processability issue and to provide adjustable drug release rates from the printed dispersions. Solid dispersions of felodipine, the model drug, were successfully fabricated using FDM 3D printing with polymer blends of PEG, PEO and Tween 80 with either Eudragit E PO or Soluplus. As PVA is one of most widely used polymers in FDM 3D printing, a PVA based solid dispersion was used as a benchmark to compare the polymer blend systems to in terms processability. The polymer blends exhibited excellent printability and were suitable for processing using a commercially available FDM 3D printer. With 10% drug loading, all characterization data indicated that the model drug was molecularly dispersed in the matrices. During in vitro dissolution testing, it was clear that the disintegration behavior of the formulations significantly influenced the rates of drug release. Eudragit EPO based blend dispersions showed bulk disintegration; whereas the Soluplus based blends showed the 'peeling' style disintegration of strip-by-strip. The results indicated that interplay of the miscibility between excipients in the blends, the solubility of the materials in the dissolution media and the degree of fusion between the printed strips during FDM process can be used to manipulate the drug release rate of the dispersions. This brings new insight into the design principles of controlled release formulations using FDM 3D printing.

## **Key words:**

FDM 3D printing, solid dispersions, hot melt extrusion, poorly soluble drugs, polymer blends

## **Abbreviations**

FDM	Fused Deposition Modeling
3D	Three Dimensional
PVA	Polyvinyl Alcohol
PLA	Poly lactide
PCL	Polycaprolactone
HPC	Hydroxypropyl Cellulose
PEG	Polyethylene Glycol
PEO	Polyethylene Oxide
DSC	Differential Scanning Calorimetry
MTDSC	Temperature Modulated Differential Scanning Calorimetry
ATR-FTIR	Attenuated Total Reflectance Fourier Transform Infrared
PXRD	Powder X-Ray Diffraction
SEM	Scanning Electron Microscopy
HME	Hot Melt Extrusion
BCS	Biopharmaceutics Classification System
T <sub>g</sub>	Glass Transition Temperature
TGA	Thermal Gravimetric Analysis
USP	United State Pharmacopoeia
APIs	Active Pharmaceutical Ingredients
UV–VIS	Ultraviolet-Visible

## Introduction

An encouraging trend of using 3D printing in pharmaceutical manufacturing has been established by the approval of Spritam<sup>®</sup>, which is the first FDA approved 3D printed oral dosage form. This first 3D printed commercial drug product used ZipDose<sup>®</sup> technology, which is a wet power deposition 3D printing method. There is a wide range of 3D printing technologies that operate via thermal or solvent evaporation mechanisms. FDM 3D printing is a thermal based 3D printing technique and has recently attracted the interest of researchers in many fields including pharmaceutical formulations design [1-3], food technology [4], and tissue engineering [5]. For pharmaceutical applications, this technique has been identified as holding future promise for developing individualized oral medicines [1-3,6-8]. FDM 3D printing can play an important role in reducing the complexity of drug regimens through incorporation of multiple drugs into a ‘polypill’ type of formulations. It may also allow different release profiles of the drug to be obtained through changing the exposed surface area or the geometry of the dosage form and through using more than one kind of carrier material with different drug release characteristics [7, 8]. Although industrial scale FDM 3D printing is used in other sectors, until now its applications in pharmaceutical manufacturing have been limited to laboratory scale. One of the significant constraints for the development of pharmaceutical FDM 3D printing is the extremely limited number of FDM printable materials currently available. In most reported cases, the printing of proposed oral solids were performed using mostly PVA, PLA and PCL [7-9]. Only recently, the uses of pharmaceutical grade polymers for FDM printing of capsules and coating layers were reported [10]. This study presents an approach using polymer blends to overcome this problem and open the possibility of using pharmaceutically approved polymers in FDM printing of oral solid dosage forms. In addition, this study also demonstrates that the blends can be used to control the disintegration and drug release of the FDM printed solid dispersions.

FDM 3D printing was originally introduced during the 1980s as a branch of the additive manufacturing technology. The key element of FDM printing is the extrusion process, which allows the thermally softened material strips to be deposited in a 'writing' mode. It principally works by converting a pre-designed software digital file coding the 3D object into a real object by adding a successive series of layers of molten or semi-liquid modeling material. Premade filaments with a specific diameter are needed for feeding into the printer. The modeling material in the printing state is pushed through a temperature-controlled 3D printing nozzle having certain diameter at a pre-adjusted speed into a temperature controlled building platform. Depending on the dimensions of the object, the printer nozzle moves in the X-Y plane in a particular pattern (determined by the shape of the object) creating the first layer. Successive layers are printed by moving either the nozzle or the platform through the Z plane with a distance equivalent to the layer thickness. The temperature of the platform is normally less than that of the extrusion head allowing the printed material to solidify between each layer [11]. The nature of the current state-of-art FDM printing technique leads to three significant barriers to exploiting its application in pharmaceutical solids production: (1) premade filaments are required as an additional process step and currently available filament extruders are largely single screw extruders which may not be able to provide sufficient compounding and mixing between the active ingredients and the excipients. Therefore, some researchers have used either a commercially available single screw filament maker or twin screw hot melt extrusion to produce the filaments for printing [7-10, 12, 13]. (2) Currently there is no effective extrusion element in commercially available FDM 3D printers instead they rely on rollers at the top of the printer to push the molten materials to the printer nozzle. Rheologically this requires the material used to have a low melt viscosity at the printing temperature. (3) The molten materials need to solidify rapidly to allow the rapid deposition

and accurate buildup of the 3D object according to the pre-set digital design [11]. This requires the printing materials to be highly thermoplastic whereas most pharmaceutical grade polymers are not thermoplastic.

The last two limitations of the technology can be overcome by selecting appropriate polymers. Polymers such as PVA, PLA and PCL have sufficient thermoplasticity to make them suitable for FDM 3D printing. However, many printable grades of these polymers are not pharmaceutical grade excipients. In addition use of these few polymers often provides little flexibility in tailoring the drug release profiles and limits the application of any delivery system produced from them. Recently the addition of plasticizers to improve the processability of controlled release polymers such as HPC and Eudragit RL and RS during FDM printing has been reported [10, 12]. However, to the best of our knowledge so far there is no report on the use of polymer blends to FDM print solid dispersions for the dissolution enhancement for poorly soluble drugs.

Formulations fabricated using FDM 3D printing are mostly solid dispersion based formulations [7-9,13]. Solid dispersions are widely used formulations for improving the dissolution of poorly water-soluble drugs [14, 15]. Molecular dispersions in which the crystalline drug is dispersed in the polymeric matrices on a molecular scale have been recognized as being highly effective for improving the dissolution and subsequent bioavailability of many poorly soluble drugs [16, 17]. This study used a BCS class II drug [18], felodipine, as a model poorly soluble drug to develop FDM 3D printable blends made of pharmaceutically approved excipients. PVA was used as the benchmark polymer in this study because of its excellent thermoplasticity and FDM printability [1, 8]. Eudragit EPO and Soluplus both have been widely used in pharmaceutical HME indicating their good

thermostability and extrudability. However, they are not FDM printable on their own. They were selected as the two model polymers which were compounded with an adjustable mixture of PEG /PEO and/or Tween 80. PEG has low melt viscosity and was used to adjust the printability of the blends. As a result of its high molecular weight, PEO provides mechanical flexibility to the filaments to allow easy feeding into the FDM printer. Tween 80 was used primarily as a plasticizer in order to lower the processing temperature to safe temperatures and to overcome degradation issues for the drug under investigation. The secondary functions of PEG, PEO and Tween 80 are associated with their good solubilizing properties for poorly water soluble drugs and plasticizing characteristics for solid dispersion mixtures [19-21].

## **Materials and methods**

### *Materials*

Felodipine, the model drug, with mean particle size of 200  $\mu\text{m}$  was purchased from Afine Chemicals Ltd (Hangzhou, China). Polyethylene glycol (PEG) (average MWT = 4000) was purchased from Sigma Aldrich (Poole, UK). Polysorbate (Tween<sup>®</sup> 80) was purchased from Acros Organics (Geel, Belgium), Polyethylene Oxide (POLYOX WSR N10 LEO) MWT= 100,000, Soluplus, Eudragit<sup>®</sup> EPO and 33-38% partially hydrolysed polyvinyl alcohol (PVA) MWT= 18,000-25,000 were kindly donated by Colorcon Ltd. (Dartford, UK), BASF (Ludwigshafen, Germany), Evonik industries (Darmstadt, Germany) and Kuraray Co., Ltd. (Tokyo, Japan), respectively. The chemical structures of the materials are listed in Supplementary Information Figure S1.

### *Preparation of placebo and felodipine loaded FDM filaments using HME*

Placebo and 10% w/w felodipine FDM filaments consisting of three sets of excipient mixtures (compositions are shown in Table 1) were prepared using a co-rotating twin-screw extruder (Haake MiniLab II Micro Compounder, Thermo Electron, Karlsruhe, Germany). The formulations containing Eudragit EPO, Soluplus and PVA as the main matrix materials are labelled with the abbreviations of CME, CMS and CMV, respectively. All ingredients were accurately weighed and premixed using a mortar and pestle for 2 minutes. For each extrusion experiment, 7 g of the premixed blend was fed into the extruder and 3 g was kept for the characterization of the physical mixtures. The extrusion was performed at the specified extrusion temperature (Table 2) with 5 minutes retention time and 100 rpm screw speed. After decreasing the rotation speed of the screws to 25 rpm the extruded soft mass of the blends was flushed directly through a metal attachment with a circular die of a diameter 1.75 mm onto a conveyer belt to produce placebo and 10% w/w felodipine loaded filaments.

#### *Using FDM 3D printing to fabricate solid dispersions*

A MakerBot Replicator II desktop 3D printer (New York, United States) equipped with 2 thermal extruding nozzles (diameter 400  $\mu\text{m}$ ) was used for printing the prepared placebo and medicated filaments. The digital file for the selected 3D shape in STL (stereolithography) format was designed using Blender software [22] and printed using MakerBot MakerWare™. In this study, a model disc shape with dimensions of 12 mm diameter and 0.6 mm thickness and was used as a standard shape to compare the characteristics of different mixtures. Printing was performed using an extrusion temperature of 150 °C without heating the platform. The 3D object was printed using standard mode with 0.2 mm layer thickness and 100% infill. The time required to complete printing each disc was  $24.7 \pm 0.1$  seconds with only small weights variation between prints (Supplementary Information Table S1). The

images of the produced 3D printed discs with their corresponding filaments are shown in Figure 1.

#### *Characterization of FDM 3D printed solid dispersions*

##### *Thermal Gravimetric Analysis (TGA)*

TGA Q5000 (TA Instruments, Newcastle, USA) was used to assess the thermal stability of the raw materials to ensure that all formulations were processed below the degradation temperature and to test the moisture content of the processed samples. 5-10 mg of each sample was loaded into the instrument and a temperature programme of 10 °C/min was used over the temperature range 25-500 °C. Each sample was tested in duplicate and Universal Analysis software was used to analyze the obtained results.

##### *Differential Scanning Calorimetry (DSC) and Temperature Modulated DSC (MTDSC)*

A Q-2000 MTDSC (TA Instruments, Newcastle, USA) equipped with (RC90) cooling unit was used to analyze felodipine matrices using standard DSC and MTDSC modes. For standard DSC, a temperature program a heating ramp of 10 °C/min was used. MTDSC experiments were also performed using a 2 °C/min heating rate, 60 sec period and 1 °C or 0.318 °C amplitude (depending on the sample) to detect the glass transition temperature(s) ( $T_g$ ) of the different formulations. Sample weights were 2-3 mg contained in an aluminum standard TA crimped pans and lids (TA Instruments, Newcastle, USA). Universal Analysis software was used to analyze the obtained results. All analyses were performed with 2-3 replicates for each sample.

##### *Attenuated total reflectance Fourier transform infrared spectroscopy (ATR-FTIR)*

All experiments were conducted using an IFS 66/S FTIR spectrometer (Bruker Optics Ltd, Coventry, UK) fitted with a Golden Gate<sup>®</sup> ATR accessory with temperature controllable top plate (Orpington, UK) equipped with diamond internal reflection element. ATR-FTIR spectra, in absorbance mode, were obtained using a scanning resolution of 2 cm<sup>-1</sup> and 32 scans for each sample in the range of wave numbers of 4000-550 cm<sup>-1</sup>. All spectra were analyzed using OPUS software.

#### *Scanning Electron Microscopy (SEM)*

A JSM 5900LV Field Emission Scanning Electron Microscope (Jeol Ltd, Japan) equipped with a tungsten hairpin electron gun was used to study the microstructure of different placebo and felodipine loaded filaments and discs. Cross sections of all samples were prepared by cutting the samples after dipping them into liquid nitrogen. All samples were attached to SEM stubs using double adhesive tape and then coated with gold using a Polaron SC7640 sputter gold coater (Quorum Technologies, city, country) prior to imaging.

#### *Powder X-Ray diffraction (PXRD)*

A Thermo ARL Xtra X-ray diffractometer (Thermo Scientific, Switzerland) with a copper X-ray Tube ( $\lambda = 1.540562 \text{ \AA}$ ) was used for to study the physical form of the drug in the different formulations and the possible changes in the nature of the components due to processing. The samples were analysed using an X-ray beam with voltage of 45 kV and a current of 40 mA. The angular scan range was ( $5^\circ < 2\theta < 60^\circ$ ) using a step scan mode with step width of 0.01° and scan speed of 1 sec/step.

#### *X-Ray Micro-Computed tomography (X $\mu$ CT)*

A SkyScan1172 high-resolution X-ray micro computed tomography (X $\mu$ CT) scanner

(Bruker-microCT, Kontich, Antwerp, Belgium) was used to 3D visualize the microstructure of the most promising blend (Eudragit EPO based filaments and FDM 3D printed discs). Placebo and 10% w/w loaded samples were scanned using an aluminium filter to cut-off high energy X-rays at an isotropic voxel resolution of 3  $\mu\text{m}$  over a total of 20 min acquisition time and a subsequent image reconstruction time of approximately 20 min per sample, using the NRecon program (version 1.6.8.0, Bruker-microCT). The collected data were then analysed using CTan and CTvol software in which the images for a small section (designated as a region of interest ROI) of each sample are converted to binary images followed by thresholding areas of different electron densities and represented in 3D models [23].

#### *Drug solubility measurements*

The saturated solubilities of felodipine were experimentally measured in the pH 6.8 PBS and pH 1.2 HCl dissolution media used in this study. The values were determined by adding an excess amount of felodipine powder (50 mg) to 25 ml of each medium. The samples (3 replicates for each) were equilibrated in a shaking incubator (MaxQ 4000, Thermo Scientific, USA) for 48 hours at 37 °C. All measurements were repeated 6 times.

#### *In vitro drug release studies*

The *in vitro* drug release profiles were measured in dissolution testing apparatus (Caleva 8ST, Germany) using the paddle method (USP apparatus 1). A paddle rotation speed of 100 rpm and 900 ml of pH 1.2 HCl (simulated gastric fluid without enzymes) or phosphate buffer pH 6.8 (simulated intestinal fluid without enzymes) at  $37\pm 0.5$  °C were used for all measurements. The pure crystalline drug (approximately 5mg in powder form) and disc shaped dispersions containing the equivalent of the daily dose (5 mg) of the drug were used in this study. Under non-sink conditions, 5ml dissolution samples were withdrawn at pre-determined time intervals. The samples were directly filtered through a membrane filter with 0.45  $\mu\text{m}$  pore

size (Minisart NML single use syringe, Sartorius, UK). The filtered sample solutions were diluted with equal volume of ethanol. 5ml of fresh pre-warmed ( $37 \pm 5$  °C) dissolution media was added to the dissolution vessel after each sampling. The samples were analysed using a UV–VIS spectrophotometer (Perkin-Elmer lambda 35, USA) at 363 nm. All dissolution tests were performed under non-sink conditions with no addition of surfactants in the media, in order to minimise the effect of polymer-surfactant interactions on the drug release behaviour from the formulations. All drug release studies were conducted in triplicate.

#### *Determination of drug loading efficiency*

Accurately weighed drug loaded FDM printed discs of different formulations were dissolved in a beaker containing 200 ml of 50:50 simulated gastric fluid pH 1.2 and absolute ethanol. The beaker was covered with a parafilm tape to minimize solvent evaporation during dissolution. The medium was stirred using magnetic stirrer at room temperature. After complete dissolution, 5 ml samples were withdrawn and filtered using 0.45  $\mu\text{m}$  pore size (Minisart NML single use syringe, Sartorius, UK). The filtered samples then scanned for their content of felodipine using a UV–VIS spectrophotometer (Perkin-Elmer lambda 35, USA) at 363 nm. The loading efficiency measurements for the loaded discs were carried out in triplicate.

## **Results**

#### *Prediction of excipient-excipient and drug-excipient miscibilities using solubility parameter ( $\delta$ ) calculations*

The miscibility between the materials used in the blends can significantly affect the processability and the qualities, such as the hardness and friability, of the finished products [24]. Therefore, predictions of the material's miscibility and likelihood of phase separation

for the three sets of blend formulation were performed. Hoy and Hoftyzer-Van Krevelen group contribution methods were used to carry out the solubility parameter calculations (detailed calculation can be found in Supplementary Information) [25, 26]. The average values obtained from the two calculations were used for comparison in order to ensure more accurate results [26]. The rule of thumb for estimating miscibility reported in literature is a difference in solubility parameter ( $\Delta\delta$ ) of less than 7 (MJ/m<sup>3</sup>)<sup>1/2</sup> indicates that the substances are miscible; a  $\Delta\delta$  value more than 10 (MJ/m<sup>3</sup>)<sup>1/2</sup> predicts unfavourable interaction and immiscibility between the components of the blend leading to phase separation. A  $\Delta\delta$  value of 7-10 (MJ/m<sup>3</sup>)<sup>1/2</sup> indicates partial miscibility of the ingredients [21, 27]. As seen in Table 3, the calculated solubility parameters for Soluplus and the processing aid materials, PEG, PEO and Tween 80, are nearly identical, indicating excellent miscibility of all excipients in CMS placebo. The  $\Delta\delta$  value is less than 4 for Eudragit with PEO, PEG and Tween 80 which also indicates good miscibility between excipients used in CME dispersions. However, the  $\Delta\delta$  value of PVA with Tween 80 is greater than 7 suggesting partial miscibility of these two excipients for CMV formulations. Based on the ranking of the  $\Delta\delta$  values, the highest miscibility of felodipine with the individual excipients is expected to be in the order of Soluplus  $\approx$  PEG 4000  $\approx$  PEO  $\approx$  Tween 80 > Eudragit EPO > PVA. This leads to the predicted the rank of the miscibility of felodipine in FDM printed formulations being CMS > CME > CMV.

#### *Processability of polymer blend based solid dispersions by FDM*

Eudragit EPO and Soluplus have been widely reported for the preparation of HME solid dispersions for enhancing the dissolution of poorly soluble drugs [28-31]. Although both polymers on their own are HME extrudable, neither of them were FDM printable even with the addition of drug. After blending with PEG, PEO and Tween 80, both polymers were FDM

printable. However, due to the higher melting viscosity and lower  $T_g$  of Eudragit than Soluplus, a greater quantity of PEG and reduced quantity of Tween 80 were added to the CME blends in comparison to CMS blends (Table 1). The PVA used in this study was 33-38% hydrolysed and the HME filament was brittle and not suitable for FDM printing. Therefore, Tween 80 was added to plasticise this material and improve the flexibility of the filaments which made feeding of the FDM printer easier.

The PVA based filaments are highly thermoplastic. As seen in Table 2, the low extrusion torques during HME indicating low melt viscosity of the materials, but readily formed the required shape upon cooling (Figure 1). For Eudragit based blends, the addition of felodipine, plasticized the mixtures and reduced the extrusion torque during HME which allowed FDM printing. For Soluplus based blends, the plasticization effect of the drug is not significant and may be masked by the higher Tween 80 content in these blends in comparison to Eudragit based blends. Although both Eudragit and Soluplus based blends gave higher extrusion torque during HME, the mixtures were FDM printable. Moreover, no clear deformation of the shape at a micron scale can be observed using SEM (Figure 2). The surface roughness at the edges of each deposited strips of CMS is slightly higher than CME and CMV. This may be attributed to the combination of suitable viscosity for FDM deposition but poor thermoplasticity. The edge of each printed strip of the materials can be easily identified. It is noted that for all three formulations the road width of each strip is approximately  $370 \pm 10$   $\mu\text{m}$  instead of  $400 \mu\text{m}$  which is the diameter of the printing nozzle. The uniformity of the small shrinkage of the road width of the printed materials indicates the similar thermal flow behavior of the three blends.

X $\mu$ CT was used to study the morphology and internal microstructure of the FDM samples at

the hundreds of microns to the mm scale. Representative X $\mu$ CT results for the placebo and 10% loaded filaments and FDM printed discs of CME blend show some level of micron scale surfaces roughness, which matches the SEM observations (Figure 3). The road width of the individual FDM strip also matches those observed in the SEM images. Small air pockets distributed inside the FDM printed discs can be seen which is absent in the HME filaments. The small air pockets are likely to be introduced during the deposition of each layer of strips. It was noted that for both HME filaments and FDM printed discs, some phase separated particles with high electron density are observed. It can be confirmed that they are not drug particles as they are also present in the placebo filaments and discs. They may be metal contamination introduced during the extrusion/3D printing processes or some inorganic additives included in the raw polymers [23].

#### *Loading efficiency of FDM printed felodipine solid dispersions*

It was reported in the literature that the drug loading efficiency of the FDM 3D printed samples prepared by passive diffusion of the drug from its organic solution into the ready-made placebo PVA filaments was often lower than the theoretical value by more than 15% [8, 32, 33]. Using a high printing temperature also can lead to unsatisfactory loading efficiency due to the thermal degradation of the drug [8, 32, 33]. A temperature of 150 °C was used in this study during the FDM printing. The loading efficiencies of felodipine in the 3D printed CMS, CME and CMV discs were 95.75 $\pm$  0.66%, 94.62  $\pm$  0.56% and 86.23  $\pm$  0.83%, respectively. This suggests that processing the mixtures using HME with subsequent FDM 3D printing at a suitable temperature can produce solid dispersions with high loading efficiency [34]. In addition, this result also indicates that the 3D printing process at 150 °C led to no thermal degradation of the active drug which was confirmed by the results obtained by TGA (Supplementary Information Figures S2 and S3). The lower loading efficiency for

10% CMV than CME and CMS may be attributed to the large particle size of PVA granules used during preparation which led to poor mixing with the Tween 80 and the drug.

#### *Physical characterization of the FDM printed solid dispersions*

Thermal transitions for the raw materials used in the various formulations were measured using DSC and are summarized in Figure 4a. The  $T_g$ s of Eudragit EPO, Soluplus, PVA, and Tween 80 were identified at  $46.7 \pm 1.0$ ,  $74.1 \pm 0.3$ ,  $45.3 \pm 0.2$ , and  $-63.9 \pm 0.2$ , respectively. The melting of other blend excipients including Tween 80 (after crystallization at  $-44.1 \pm 0.6$  °C), PEG and PEO and the model drug can also be identified at  $-9.1 \pm 0.4$ ,  $65.6 \pm 0.1$ ,  $59.6 \pm 0.2$  °C and  $144.7 \pm 0.0$  °C, respectively. The physical mixtures of the CME and CMS show melting of PEG and PEO, but no melting of the model drug (Figure 4b). This is likely to be due to the thermal dissolution effect of the crystalline drug in the polymer mixtures [20]. The melting of felodipine is evident in the DSC results of the physical mixtures of CMV. This confirms the partial miscibility between felodipine and PVA predicted previously. MTDSC was used to further investigate the  $T_g$  region of the samples. As seen in Figure 5a, the MTDSC results of the physical mixtures of CME show no detectable  $T_g$ . A  $T_g$  at approximately  $-55$  °C can be detected for the physical mixtures of CMS which probably arises from the mixture of PEG/PEO/Tween 80. Two  $T_g$ s can be clearly seen at  $-55.4 \pm 0.2$  and  $39.4 \pm 4.3$  °C in the MTDSC results of the physical mixtures of CMV blends. As the first  $T_g$  is higher than the  $T_g$  of pure Tween and the second is lower than the  $T_g$  of pure PVA, they are likely to be the  $T_g$ s of Tween-drug and PVA-moisture phases, respectively. These  $T_g$ 's shift to higher temperature ( $-51.8 \pm 0.3$  °C and  $42.9 \pm 4.45$  °C) in the reheating cycle which may be caused by the further mixing of Tween 80 and PVA and moisture loss of the main PVA phase, respectively (Figure 5c).

In FDM printed CME and CMS discs containing 10% felodipine, DSC shows the joint melting of crystalline PEG and PEO. The melting enthalpy values of the crystalline PEG-PEO were similar in CME and CMS. However, it should be mentioned that there was 30% w/w PEG-PEO in CME and 25% in CMS. This indicates that a greater amount of the crystalline PEG-PEO phase was present in CMS in comparison to CME (Supplementary information Table S2). It was also noted that the melting point of the PEG-PEO shifted to lower temperatures in comparison to those observed in the results of their physical mixtures. The solubilisation of other excipients and felodipine may be responsible for this melting depression of the crystalline PEG-PEO phase in the printed dispersions. For the drug loaded CME, the theoretical  $T_g$  of the blend calculated using Fox equation (Supplementary Information Table S3) is  $-5.2\text{ }^\circ\text{C}$ . This agrees well with the  $T_g$  of the FDM printed CME discs measured by MTDSC which is a broad transition at approximately  $-6\text{ }^\circ\text{C}$  (Figure 5a). The detection of a single  $T_g$  is a good indicator of the formation of a molecular dispersion of the drug and the excipients in CME. For drug loaded CMS samples, the  $T_g$  of Tween 80 disappeared and no clear joint  $T_g$  can be detected by MTDSC (Figure 5b). No drug melting was detected in the DSC and MTDSC results of CMV dispersions. Two  $T_g$ s are present in the MTDSC results of the CMV dispersions (Figure 5c) indicating the phase separation in printed CMV dispersions. The  $T_g$  of the PVA phase shifts to a lower temperature ( $25.7 \pm 1.3\text{ }^\circ\text{C}$ ) in the FDM printed dispersions in comparison to the physical mixture. As the  $T_g$  of PVA is lower than amorphous felodipine and higher than Tween 80, this may indicate enhanced mixing of Tween with PVA after processing. The separate  $T_g$  at  $-51.6 \pm 2.7\text{ }^\circ\text{C}$  can be assigned to the Tween rich phase. It is likely that felodipine is molecularly dispersed in both PVA-rich and Tween 80-rich phases.

ATR-FTIR and PXRD were used to further confirm the physical states of felodipine in the

solid dispersions. As seen in Figure 6 the NH stretching peak of crystalline felodipine form I at  $3367\text{ cm}^{-1}$  is visible in the physical mixtures. This peak transforms into a broad peak with low intensity in the spectra of the FDM printed CME, CMS and CMV discs. This broadening may be caused by a combination of the formulation of molecular dispersion of felodipine and the small quantity (less than 3% w/w) of moisture present in the printed discs as shown in the TGA results (Supplementary Information Figure S4). A few signature diffraction peaks of the crystalline felodipine are present in the PXRD diffraction patterns of the physical mixes for the three blends (Figure 7). Because both CME and CMS contain semi-crystalline PEG and PEO, the main diffraction peaks of these two polymers can be seen in the PXRD patterns of the FDM printed discs. The crystalline drug related peaks completely disappear in all patterns of the 10% w/w loaded printed discs. Taking in account of the miscibility prediction of felodipine and the excipients, the phase separation of amorphous felodipine is unlikely and the results indicate the formation of felodipine molecular dispersions at the detection limit of PXRD. These results agree well with the DSC results and confirm felodipine was molecularly dispersed in all three matrices.

#### *In vitro disintegration and drug release study of FDM printed felodipine dispersions*

The saturated solubilities of crystalline felodipine in the media were  $0.14 \pm 0.14\ \mu\text{g/ml}$  and  $0.47 \pm 0.08\ \mu\text{g/ml}$  in pH 6.8 PBS and pH 1.2 HCl, respectively. Although felodipine is a neutral compound, the lower solubility of the crystalline felodipine in pH 6.8 PBS than pH 1.2 HCl observed may be attributed to the higher salt contents in PBS (with a molarity of 0.19 M) than HCl (with a molarity of 0.12 M). The dissolution rates of crystalline felodipine powder in both media were extremely slow. After 6-hour dissolution test under non-sink conditions, the amounts of dissolved crystalline felodipine did not reach saturated solubilities of the drug in both media. A significant enhancement of the dissolution profile of felodipine from CME

discs in comparison to the crystalline model drug alone was obtained when pH 1.2 HCl was used as the dissolution media (Figure 8a). The rapid release of approximately 84.3% of the drug load was achieved within 30 minutes. This dissolution improvement may be attributed to the formation of the molecular drug dispersion and the high solubility of Eudragit E PO in pH 1.2 HCl. The rapid disintegration of the CME discs can be observed within the first 5 minutes of the dissolution experiments (Figure 9). Eudragit E PO is insoluble at pH 6.8, thus little drug release from the CME was expected. However, a delayed but 100% drug release of felodipine from the CME discs in pH 6.8 PBS was obtained (Figure 8b). Less than 8% drug release occurred in the first 90 minutes. However, from 90 minutes onwards, a linear zero-order release profile with 100% drug release by 6 hours was observed. The images of the discs during the dissolution in pH 6.8 PBS show the slow bulk erosion and disintegration of the discs which was completed by 6 hours (Figure 9). A minor level of swelling of the discs prior to the complete disintegration and dissolution was observed.

CMS discs showed significantly slower drug release profile in pH 1.2 HCl than CME discs. However, it is interesting to note that some improvement in drug dissolution in comparison to the crystalline drug alone was still observed from 1 hour onwards and the release follows a linear release pattern. The maximum release of 28% was achieved after 6 hours in vitro dissolution. Although Soluplus has been reported to be a water-soluble polymer, the addition of the inorganic salts in the dissolution medium can depress the cloud point of the polymer and reduce the solubility of the polymer in the media [35]. Figure 10 captures the start of the disintegration process of CMS discs between 60 to 90 minutes into the dissolution test. A closer examination of the images reveals the sequence of the disintegration of CMS discs into segments of printed strips which is significantly different from the disintegration of CME in pH 6.8 PBS. Between 60-90 minutes, the individual printed polymer strips at the outer edge

of the FDM discs started to unravel into single long strands. There were three printed layers stacked together to form the discs, the outer printed layer unravelled first to reveal the middle layers. This was followed by further breakdown of the longer polymer strips into smaller segments. This unique disintegration process contributed to the increased release of drug and led to the observed increase in the amount of drug released from 1 hour onwards (Figure 8a). This indicates that the disintegration process may be the limiting step for initiating the drug release from CMS in HCl. The linear release profile also suggests that the release kinetics of felodipine from disintegrated CMS strips is close to zero-order. In pH 6.8 PBS, CMS discs show no dissolution enhancement of felodipine despite of the formation of the molecular dispersions of the drug by HME and FDM 3D printing (Figure 8b). It was noted that no disintegration occurred in any FDM printed discs during the period of the dissolution tests in pH 6.8 PBS. The increased amount of inorganic salt in the PBS may contribute to further limit the solubility of Soluplus in the media. No significant swelling was observed through the 6 hours of dissolution and a minimal disintegration started by 6 hours (Figure 10b).

In order to further understand the release behaviour, segments of the CMS samples after 6 hours dissolution were studied using ATR-FTIR and DSC. The ATR-FTIR results (Figure 10c) show no changes of the drug and excipient peaks in comparison to the dry freshly prepared discs after 6 hours dissolution in both media. This confirms that the drug was still in amorphous dispersion with the polymer matrix. These results are consistent with the transparency of the dried matrices and the absence of drug crystals in the SEM data of these samples (Supplementary information Figure S5). However, the peaks associated with PEG, PEO and Tween 80, such as the peaks between 1500 - 850  $\text{cm}^{-1}$ , have shown significant changes in peak intensity and shape. DSC detected much smaller PEG/PEO melting peaks in the post-dissolution discs in comparison to the fresh dry sample (Figure 10d), indicating the

leaching of PEG/PEO during dissolution. The first heating cycle showed an overlapped peak of the  $T_g$  of Soluplus and dehydration of the matrix. However, the second heating cycle revealed the  $T_g$  of Soluplus. These results imply that the remaining segments after dissolution are largely Soluplus which retains the unreleased drug.

No significant release improvement of felodipine from CMV discs was observed in either pH 1.2 HCl or pH 6.8 PBS in comparison to the crystalline drug (Figure 8). The PVA used in this study was a low hydrolysis grade which led to the poor aqueous solubility of the polymer. In addition, the effect of ionic strength of the dissolution medium may also play a role in this case, reducing the dissolution of PVA in the media [36]. For both cases a degree of gelling of the discs during dissolution can be seen in Figure 11a and b. The gelation of CMV discs can be attributed to the hydrogel formation ability of PVA reported in literature [37, 38]. The discs in pH 1.2 HCl show significant softening that led to the folding of the wetted discs (which appears as reduction in size), whereas there was no change in size of the discs tested in pH 6.8 PBS. The ATR-FTIR results of the dried CMV samples are shown in Figure 11c. No changes can be observed in comparison to the dry freshly prepared discs indicating that there was no change in the state of the drug in the CMV solid dispersions after 6 hours exposure in both media. The DSC results of the dried discs after 6 hours dissolution reveal the absence of a  $T_g$  of Tween 80 which was present in the freshly prepared discs (Figure 11d). This indicates the leaching of Tween 80 during dissolution.

## **Discussion**

### ***Linking phase behavior with FDM printability of the dispersions***

Polymer blending is a widely used formulation strategy in the polymer and plastic industries to improve the processability of materials. This study tackled the FDM printability issues of two FDA approved and widely used pharmaceutical polymers, Soluplus and Eudragit EPO, by blending the polymers with a mixture of PEG, PEO and Tween 80. Although both polymers have wide applications in preparation of pharmaceutical HME dispersions, they are not printable by conventional FDM 3D printers due to their high melt viscosity and poor fluidity. The addition of the mixture of PEG, PEO, Tween 80 as well as the model drug significantly improved the viscosity of the polymers during printing as result these then matched the printing performance of the PVA based system that is one of the main matrix materials used currently in FDM 3D printing. This improved the thermal mechanical properties allowing the felodipine-loaded dispersions to be printed into disc shaped, triple layered matrices. A clear understanding of the phase behavior of the printed system is extremely important for further interpretation of the mechanism of formulation stabilization and drug release. As a result of the large number of ingredients used in the printed discs, characterization of the phase behavior of the systems is complex. This study took the simplified approach of ranking the miscibilities between excipients in order to gain some insight into the phase behavior of the blend matrices and the miscibility of felodipine with different polymer blends to allow the prediction of likelihood of the formation of molecular dispersions of the drug with polymers. The prediction revealed Soluplus and Eudragit E PO were miscible with PEG/PEO and Tween 80; whereas PVA is only partially miscible with Tween 80. Therefore the mechanism by which the printability of Soluplus and Eudragit is improved by addition of these excipients is probably the combination of improved melt viscosity and plasticization of the polymers. Results indicated the formation of a molecular dispersion of felodipine at 10% loading in FDM printed CME and CMS dispersions. Therefore drug incorporation further contributed to the plasticization of the polymer matrices.

The addition of Tween 80 reduced the stiffness of the PVA filaments and eased the printing process. The weakening of the stiffness may be attributed to the formation of discontinuous Tween 80 phases in PVA dispersions, as the two are partially miscible. The addition of felodipine further plasticized the polymer.

### ***Linking phase behavior with in vitro disintegration and dissolution performance***

The phase behavior of the printed discs is important for understanding the differences in the drug release rates of the formulations. The slower drug release from the CMS system than CME is a result of the combination of lower solubility of Soluplus than Eudragit in the media and the physical state of the excipients in the dispersions. Although both formulations were confirmed to be molecular dispersions of felodipine, their crystalline PEO/PEG contents are different. The higher crystalline PEG-PEO content in the CMS compared to CME may contribute to the slower drug release from CMS discs. This is because that the crystalline PEG/PEO required a wetting and hydration prior to dissolution; whereas these may not occur for the molecularly mixed PEG/PEO in the polymer matrices. The reason for the higher crystalline content may be associated with the higher melt viscosity of Eudragit than Soluplus as suggested by the HME processing torque values. As HME and FDM printing both were performed at temperatures above the melting point of the crystalline PEO and PEG, higher melt viscosity of the matrix polymer would be more effective in limiting the diffusion of PEG and PEO molecules to form large crystalline domains during recrystallization on cooling (post-FDM printing). However despite the fact that PEO is a well-known controlled release matrix excipient which hydrates and swells once it is in contact with aqueous media [39-42], the limited amount of swelling observed in CME and CMS discs during dissolution, indicated that the dissolution of PEO/PEG in the dispersions is the more dominant process in these

blends. The intimate mixing between PEG/PEO and Soluplus and Eudragit E PO may contribute to this observed behavior.

Another interesting feature of the dissolution behavior of these FDM 3D printed discs is the difference in their disintegration behavior, which in the case of CMS in pH 1.2 HCl and CME in pH 6.8 PBS led to the ‘switching on’ effect of the drug release (Figure 8). It indicates that the disassembly of the bulky 3D object that was fabricated by micron-size polymeric strips may be used as a novel mechanism of the drug release performance. Therefore a clear understanding of the disintegration behavior of the formulation is vitally important. In the literature, the disintegration process of FDM printed 3D matrices is still poorly understood. The results of this study revealed the unraveling of the printed strips of CMS formulation and bulk erosion behavior of CME discs. The exact mechanism for this difference is not clear, but (1) the degree of fusion between the printed strips and layers and (2) the speed of dissolution of the matrix polymer may be relevant. As seen in Figure 2, the edges of the printed strips of CMS are much rougher than CME discs. This may be an indication of low melt viscosity of the materials and rapid solidification of the materials after deposition. This should lead to the better-defined interfaces between strips and layers which may contribute to the observed ‘peeling’ effect of strip by strip during the disintegration of CMS. The higher solubility of Eudragit at pH 1.2 than Soluplus is believed to responsible to the rapid disintegration and dissolution of CME in pH 1.2. For CMS, the drug release results strongly indicated that disintegration is the limiting step for drug release. Following disintegration, controlled release of drug following zero-order kinetics was observed. The zero order release of CMS in pH 1.2 media may be explained by the small diameter of each strip segment, which contributes to the short diffusion path length of the drug molecules. This short path length led to the negligible effect of changes in diffusion length during dissolution. In addition, the

continuous slow breakdown into shorter segments can provide a constantly increasing release surface for the drug molecules and led to the observed zero-order like release profile. This brings insight into the potential of controlling the drug release rate via manipulation of the disintegration behaviour of the bulky solid formulation. This study has demonstrated that this is achievable using FDM printing technology, with careful selection of excipients.

Finally the phase behaviour can also be used to explain why the prevention of drug recrystallization in the formulations that have no drug dissolution enhancement (CMS and CMV). For CMV, as the solubility study suggested the separation of a Tween 80 rich phase and a PVA rich phase, one may expect the leaching of Tween during dissolution, which would liberate some drug. However, as extremely limited drug release was observed, it indicates that although the leaching of Tween may lead to some drug release, the majority of drug is still held as molecular dispersion in PVA matrices. This was confirmed by the DSC and ATR-FTIR results of the post-dissolution dried samples. The fact that no significant drug crystallisation occurred during the period of dissolution indicates that the polymer to drug ratio is efficient in stabilising and preventing crystallisation of the remaining drug in the matrices. This also applies to the CMS systems in which no drug recrystallization was observed during 6 hours of dissolution.

## **Conclusion**

This study demonstrated the use of polymer blends to overcome the poor printability of pharmaceutical polymers during FDM 3D printing. The solid dispersions of felodipine with Eudragit and Soluplus were successfully prepared using FDM printing after blending with the process and drug release aids, PEG, PEO and Tween 80. Distinctively different disintegration

behaviour of the 3D discs with different polymer blends allowed the manipulation of the rate of drug release. The results demonstrated the effect of the complex interplay between the miscibility of the excipients in the blends, the solubility of the polymer in the media and the formation of interfaces between printed strips during the FDM printing on drug release behaviour of the dispersions. This brings new insights into the design principles for controlled release formulations manufactured using FDM 3D printing.

### **Acknowledgement**

Muqdad Alhjjaj would like to acknowledge the Higher Committee for Education Development in Iraq (HCED Iraq) for their generous financial support for his PhD. The authors are gratefully thankful to Nick Corps from Bruker for helping with performing the XuCT measurements of the samples.

### **Reference:**

1. Skowrya J, Pietrzak K, Alhnan MA. Fabrication of extended-release patient-tailored prednisolone tablets via fused deposition modelling (FDM) 3D printing. *European Journal of Pharmaceutical Sciences*. 2015;68:11-7.
2. Goyanes A, Wang J, Buanz A, Martínez-Pacheco R, Telford R, Gaisford S, et al. 3D Printing of Medicines: Engineering Novel Oral Devices with Unique Design and Drug Release Characteristics. *Molecular Pharmaceutics*. 2015;12(11):4077-84.
3. Khaled SA, Burley JC, Alexander MR, Roberts CJ. Desktop 3D printing of controlled release pharmaceutical bilayer tablets. *International Journal of Pharmaceutics*. 2014;461(1–2):105-11.

4. Godoi FC, Prakash S, Bhandari BR. 3d printing technologies applied for food design: Status and prospects. *Journal of Food Engineering*. 2016;179:44-54.
5. Laura R-C, Andrew G, Callum F, Joel S, Kevin S, Jing Y. Characterisation of the surface structure of 3D printed scaffolds for cell infiltration and surgical suturing. *Biofabrication*. 2016;8(1):015016.
6. Jonathan G, Karim A. 3D printing in pharmaceuticals: A new tool for designing customized drug delivery systems. *International Journal of Pharmaceutics*. 2016;499(1–2):376-94.
7. Goyanes A, Robles Martinez P, Buanz A, Basit AW, Gaisford S. Effect of geometry on drug release from 3D printed tablets. *International Journal of Pharmaceutics*. 2015;494(2):657-63.
8. Goyanes A, Wang J, Buanz A, Martínez-Pacheco R, Telford R, Gaisford S, et al. 3D Printing of Medicines: Engineering Novel Oral Devices with Unique Design and Drug Release Characteristics. *Molecular Pharmaceutics*. 2015;12(11):4077-84.
9. Holländer J, Genina N, Jukarainen H, Khajeheian M, Rosling A, Mäkilä E, Sandler N. Three-Dimensional Printed PCL-Based Implantable Prototypes of Medical Devices for Controlled Drug Delivery. *Journal of Pharmaceutical Sciences*. 2016; doi: 10.1016/j.xphs.2015.12.012.
10. Melocchi A, Parietti F, Loreti G, Maroni A, Gazzaniga A, Zema L. 3D printing by fused deposition modeling (FDM) of a swellable/erodible capsular device for oral pulsatile release of drugs. *International Journal of Pharmaceutics*. 2016; 509: 255-263.
11. Chua CK, Leong KF, Lim CS. *Rapid Prototyping: Principles and Applications*: World Scientific; 2003. 129 p.

12. Pietrzak K, Isreb A, Alhnan MA. A flexible-dose dispenser for immediate and extended release 3D printed tablets. *European Journal of Pharmaceutics and Biopharmaceutics*. 2015;96:380-7.
13. Sandler N, Salmela I, Fallarero A, Rosling A, Khajeheian M, Kolakovic R, et al. Towards fabrication of 3D printed medical devices to prevent biofilm formation. *International Journal of Pharmaceutics*. 2014;459(1–2):62-4.
14. Pina MF, Zhao M, Pinto JF, Sousa JJ, Craig DQM. The Influence of Drug Physical State on the Dissolution Enhancement of Solid Dispersions Prepared Via Hot-Melt Extrusion: A Case Study Using Olanzapine. *Journal of Pharmaceutical Sciences*. 2014;103(4):1214-23.
15. Fong SYK, Ibisogly A, Bauer-Brandl A. Solubility enhancement of BCS Class II drug by solid phospholipid dispersions: Spray drying versus freeze-drying. *International Journal of Pharmaceutics*. 2015;496(2):382-91.
16. Yang Z, Nollenberger K, Albers J, Craig D, Qi S. Microstructure of an Immiscible Polymer Blend and Its Stabilization Effect on Amorphous Solid Dispersions. *Molecular Pharmaceutics*. 2013;10(7):2767-80.
17. Sarode AL, Malekar SA, Cote C, Worthen DR. Hydroxypropyl cellulose stabilizes amorphous solid dispersions of the poorly water soluble drug felodipine. *Carbohydrate Polymers*. 2014;112:512-9.
18. Patil PR, Biradar SV, Paradkar AR. Extended Release Felodipine Self-Nanoemulsifying System. *AAPS PharmSciTech*. 2009;10(2):515-23.
19. Regardh CG, Edgar B, Olsson R, Kendall M, Collste P, Shansky C. Pharmacokinetics of felodipine in patients with liver disease. *Eur J Clin Pharmacol*. 1989;36(5):473-9.

20. Alhijaj M, Bouman J, Wellner N, Belton P, Qi S. Creating Drug Solubilization Compartments via Phase Separation in Multicomponent Buccal Patches Prepared by Direct Hot Melt Extrusion-Injection Molding. *Mol Pharm.* 2015;12(12):4349-62.
21. Ghebremeskel AN, Vemavarapu C, Lodaya M. Use of surfactants as plasticizers in preparing solid dispersions of poorly soluble API: Selection of polymer–surfactant combinations using solubility parameters and testing the processability. *International Journal of Pharmaceutics.* 2007;328(2):119-29.
22. Adamkiewicz M, Rubinsky B. Cryogenic 3D printing for tissue engineering. *Cryobiology.* 2015;71(3):518-21.
23. Alhijaj M, Yassin S, Reading M, Zeitler JA, Belton P, Qi S. Characterization of Heterogeneity and Spatial Distribution of Phases in Complex Solid Dispersions by Thermal Analysis by Structural Characterization and X-ray Micro Computed Tomography. *Pharmaceutical Research.* 2016:1-19.
24. Baird JA, Taylor LS. Evaluation of amorphous solid dispersion properties using thermal analysis techniques. *Advanced Drug Delivery Reviews.* 2012;64(5):396-421.
25. Hoy KL, Union Carbide C, Solvents, Coatings Materials D, Research, Development D. The Hoy tables of solubility parameters. South Charleston, W. Va.: Union Carbide Corp., Solvents & Coatings Materials, Research & Development Dept.; 1985.
26. Van Krevelen DW, Te Nijenhuis K. Properties of polymers. 4th ed. Oxford, UK: Elsevier Scientific Publication; 2009. 189-227 p.
27. Prasad D, Chauhan H, Atef E. Amorphous Stabilization and Dissolution Enhancement of Amorphous Ternary Solid Dispersions: Combination of Polymers Showing Drug–Polymer

Interaction for Synergistic Effects. *Journal of Pharmaceutical Sciences*. 2014;103(11):3511-23.

28. Kalivoda A, Fischbach M, Kleinebudde P. Application of mixtures of polymeric carriers for dissolution enhancement of oxeiglitaraz using hot-melt extrusion. *International Journal of Pharmaceutics*. 2012;439(1–2):145-56.

29. Liu J, Cao F, Zhang C, Ping Q. Use of polymer combinations in the preparation of solid dispersions of a thermally unstable drug by hot-melt extrusion. *Acta Pharmaceutica Sinica B*. 2013;3(4):263-72.

30. Sarode AL, Sandhu H, Shah N, Malick W, Zia H. Hot melt extrusion (HME) for amorphous solid dispersions: Predictive tools for processing and impact of drug–polymer interactions on supersaturation. *European Journal of Pharmaceutical Sciences*. 2013;48(3):371-84.

31. Jijun F, Lishuang X, Xiaoli W, Shu Z, Xiaoguang T, Xingna Z, et al. Nimodipine (NM) tablets with high dissolution containing NM solid dispersions prepared by hot-melt extrusion. *Drug Development and Industrial Pharmacy*. 2011;37(8):934-44.

32. Goyanes A, Buanz ABM, Basit AW, Gaisford S. Fused-filament 3D printing (3DP) for fabrication of tablets. *International Journal of Pharmaceutics*. 2014;476(1–2):88-92.

33. Goyanes A, Buanz ABM, Hatton GB, Gaisford S, Basit AW. 3D printing of modified-release aminosalicylate (4-ASA and 5-ASA) tablets. *European Journal of Pharmaceutics and Biopharmaceutics*. 2015;89:157-62.

34. Park J-B, Kang C-Y, Kang W-S, Choi H-G, Han H-K, Lee B-J. New investigation of distribution imaging and content uniformity of very low dose drugs using hot-melt extrusion method. *International Journal of Pharmaceutics*. 2013;458(2):245-53.

35. Hughey JR, Keen JM, Miller DA, Kolter K, Langley N, McGinity JW. The use of inorganic salts to improve the dissolution characteristics of tablets containing Soluplus®-based solid dispersions. *European Journal of Pharmaceutical Sciences*. 2013;48(4–5):758-66.
36. De Jaeghere W, De Beer T, Van Bocxlaer J, Remon JP, Vervaet C. Hot-melt extrusion of polyvinyl alcohol for oral immediate release applications. *International Journal of Pharmaceutics*. 2015;492(1–2):1-9.
37. Jiang S, Liu S, Feng W. PVA hydrogel properties for biomedical application. *Journal of the Mechanical Behavior of Biomedical Materials*. 2011;4(7):1228-33.
38. Jensen BEB, Dávila I, Zelikin AN. Poly(vinyl alcohol) Physical Hydrogels: Matrix-Mediated Drug Delivery Using Spontaneously Eroding Substrate. *The Journal of Physical Chemistry B*. 2016.
39. Colombo P, Bettini R, Santi P, Peppas NA. Swellable matrices for controlled drug delivery: gel-layer behaviour, mechanisms and optimal performance. *Pharmaceutical Science & Technology Today*. 2000;3(6):198-204.
40. Li H, Hardy RJ, Gu X. Effect of Drug Solubility on Polymer Hydration and Drug Dissolution from Polyethylene Oxide (PEO) Matrix Tablets. *AAPS PharmSciTech*. 2008;9(2):437-43.
41. Maggi L, Bruni R, Conte U. High molecular weight polyethylene oxides (PEOs) as an alternative to HPMC in controlled release dosage forms. *International Journal of Pharmaceutics*. 2000;195(1–2):229-38.
42. Ma L, Deng L, Chen J. Applications of poly(ethylene oxide) in controlled release tablet systems: a review. *Drug Development and Industrial Pharmacy*. 2014;40(7):845-51.

**Table 1.** Composition of placebo and 10% w/w felodipine loaded FDM dispersions.

Mixture Code	Felodipine % w/w	Eudragit EPO % w/w	Soluplus % w/w	PVA % w/w	Tween 80 % w/w	PEG 4000 % w/w	PEO WSR % w/w
Placebo CME	-----	55.56	-----	-----	11.10	16.67	16.67
10% w/w CME	10	50	-----	-----	10	15	15
Placebo CMS	-----	-----	55.56	-----	16.67	11.10	16.67
10% w/w CMS	10	-----	50	-----	15	10	15
Placebo CMV	-----	-----	-----	75	25	-----	-----
10% w/w CMV	10	-----	-----	67.5	22.5	-----	-----

**Table 2.** HME-3D printing processing parameters of placebo and 10% w/w loaded felodipine filaments and 3D printed discs.

Mixture Code	HME temp. (°C)	FDM printing temp. (°C)	Extrusion torque (N.cm)
Placebo CME	100	150	24
10% w/w CME	100	150	18
Placebo CMS	120	150	7
10% w/w CMS	120	150	8
Placebo CMV	130	150	1
10% w/w CMV	130	150	1

**Table 3.** Predicted solubility parameters of components of formulation and miscibility of felodipine in different excipients and their blends.

<b>Compound</b>	<b>Hoy's <math>\delta</math> (MJ/m<sup>3</sup>)<sup>1/2</sup></b>	<b>Hoftyzer–Van Krevelen <math>\delta</math> (MJ/m<sup>3</sup>)<sup>1/2</sup></b>	<b>Average <math>\delta</math> (MJ/m<sup>3</sup>)<sup>1/2</sup></b>
Felodipine	21.08	20.60	20.84
Eudragit EPO	18.55	18.80	18.68
Soluplus	24.34	18.94	21.64
PVA	28.79	30.53	29.66
Tween 80	22.71	20.9	21.81
PEO	21.44	22.00	21.72
PEG	21.44	22.00	21.72

**Figure 1.** Images of the prepared HME filaments and 3D printed discs.

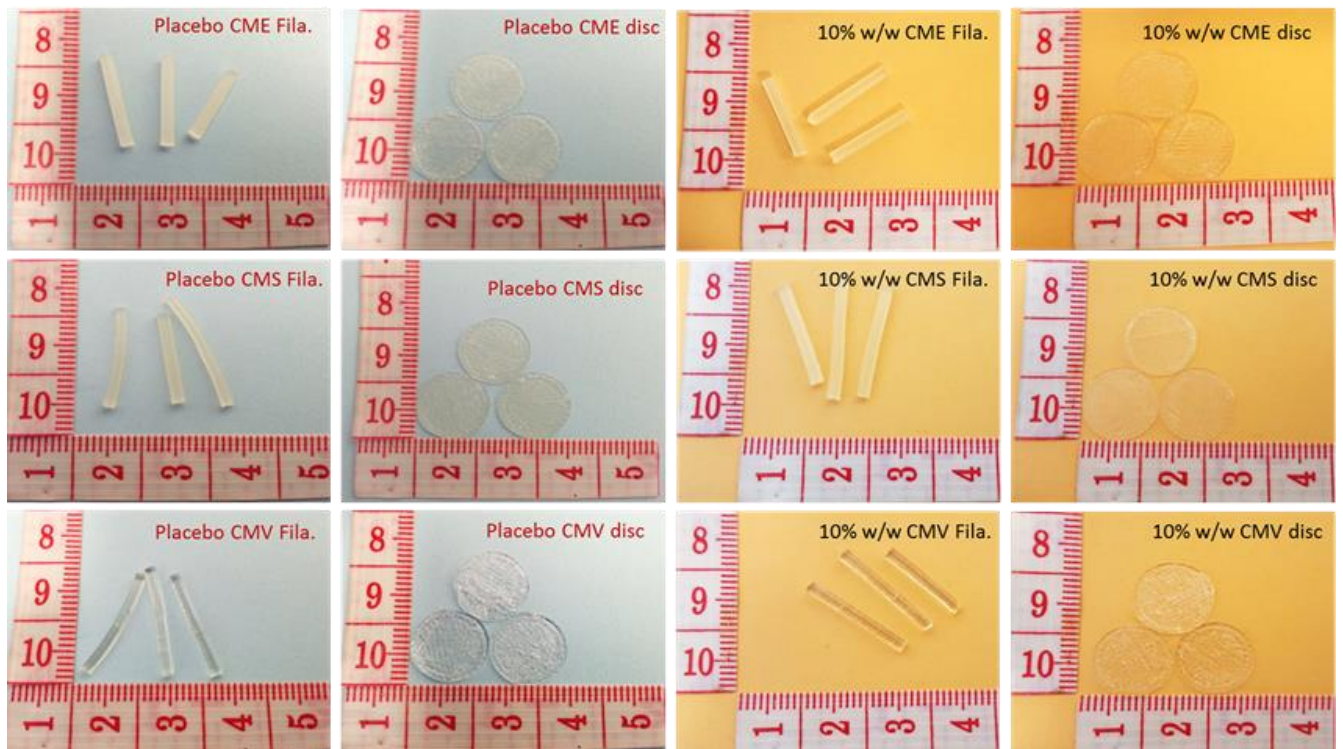


**Figure 2.** SEM images for 10% w/w felodipine loaded FDM 3D printed discs. CME (a) surface and (b) cross-section; CMS (c) surface and (d) cross-section; CMV (e) surface and (f) cross-section. The dotted lines indicate the widths of filaments strips after FDM printing.

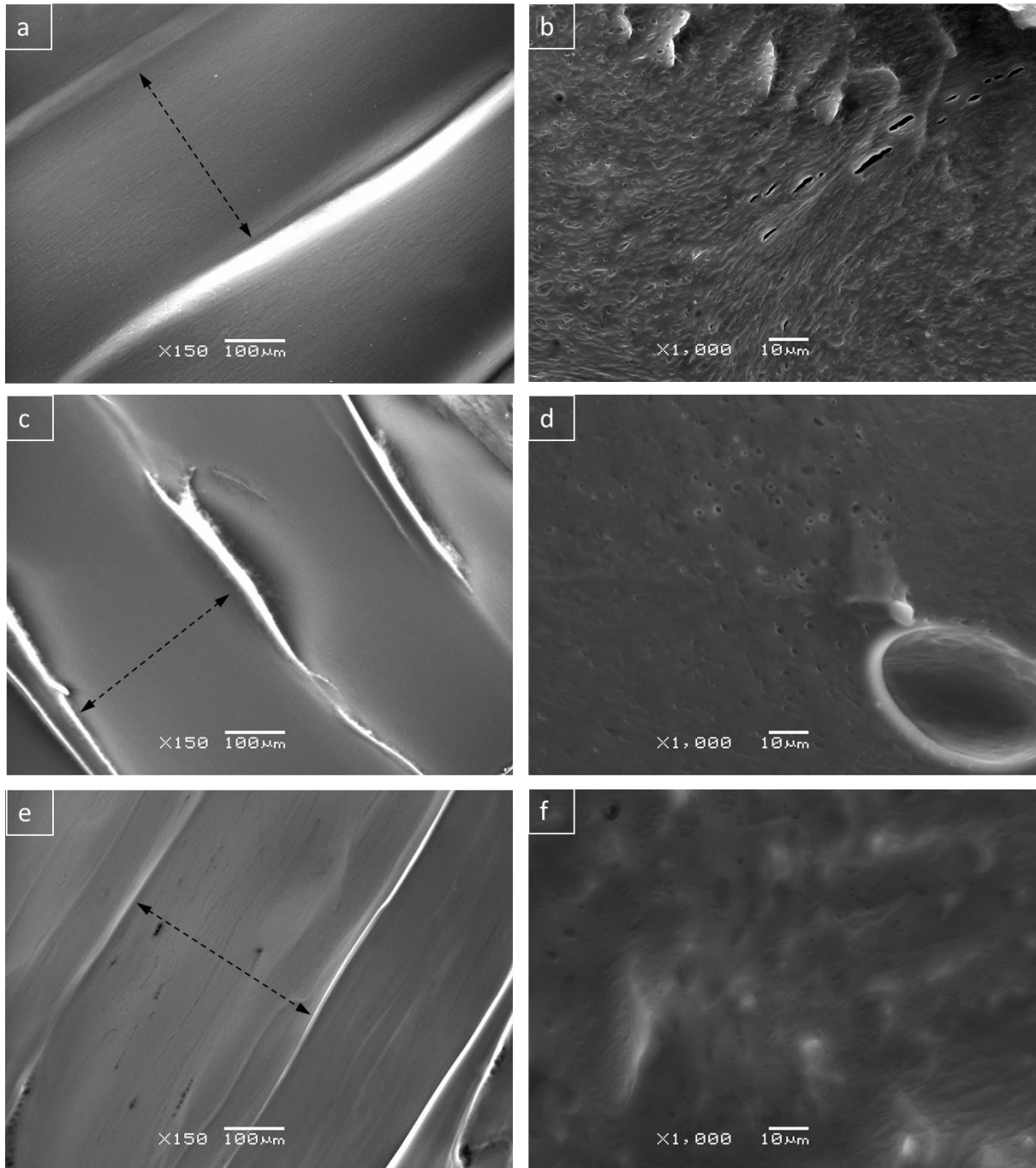


**Figure 3.** Representative X $\mu$ CT reconstructed 3D images of CME placebo and 10% w/w felodipine loaded CME discs. HME filaments (left) and FDM 3D printed discs (right). The phase separate particles are likely to be metal contaminations introduced during HME and FDM printing.

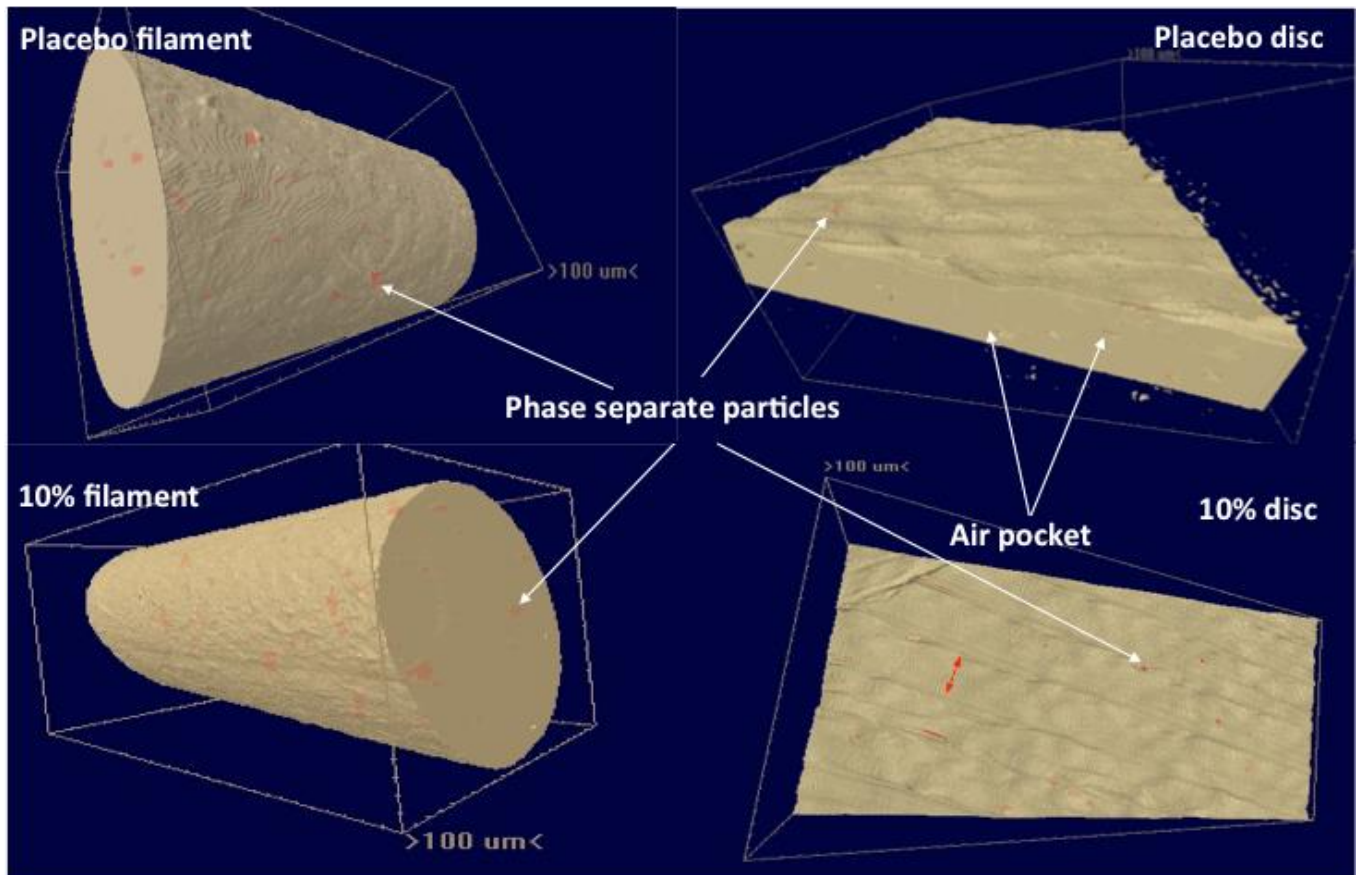


**Figure 4.** DSC thermograms illustrating different thermal events for (a) raw materials and (b) physical mixtures and FDM 3D printed discs of CME, CMS and CMV.

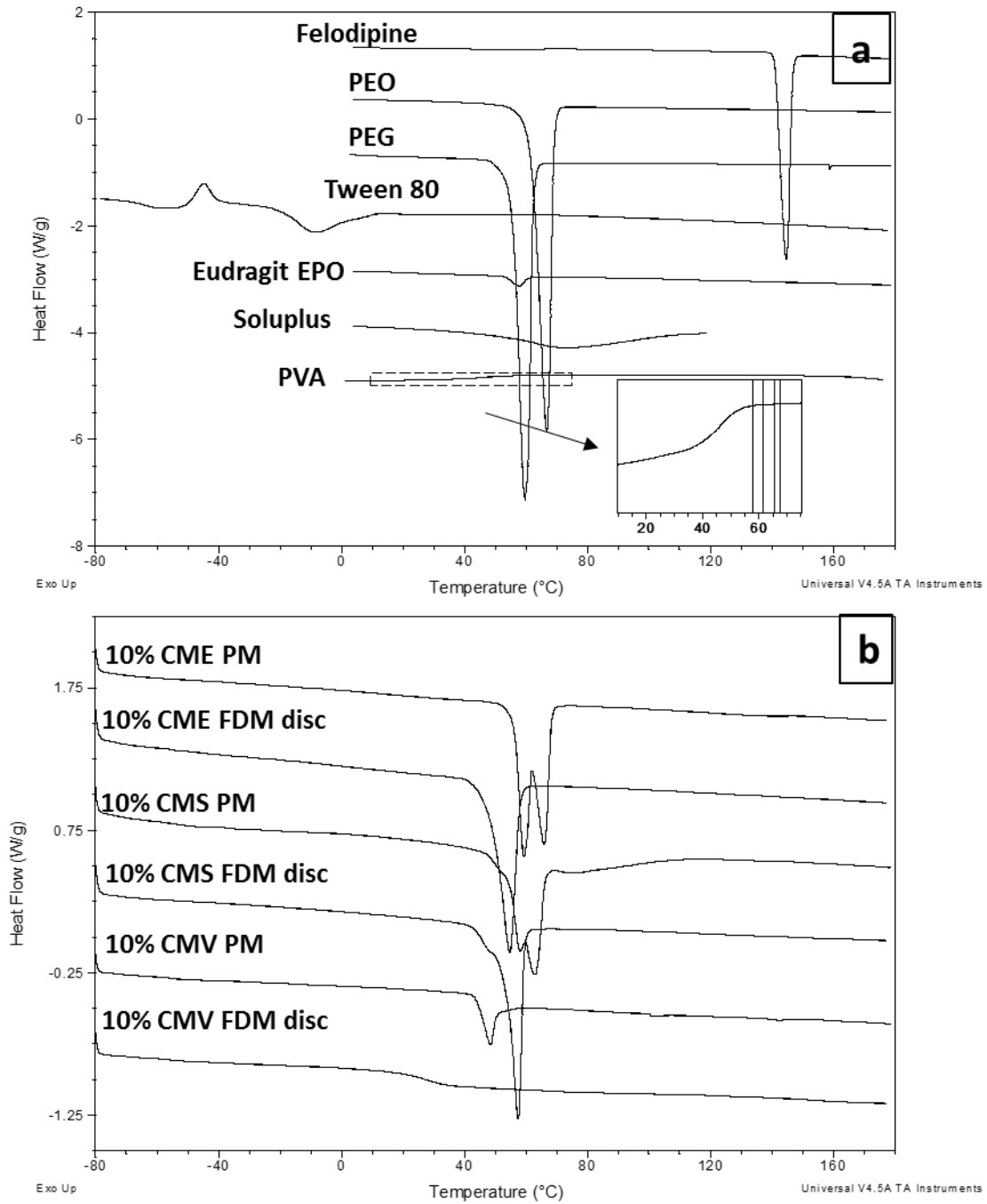


**Figure 5.** MTDSC thermograms showing the  $T_g$  of (a) CME formulations using temperature program of 1.0 °C amplitude, 60 sec period and 2 °C/ min heating rate; (b) CMS and (c) CMV mixtures using a heat only temperature program of 0.318 °C amplitude, 60 sec period and 2 °C/ min heating rate.

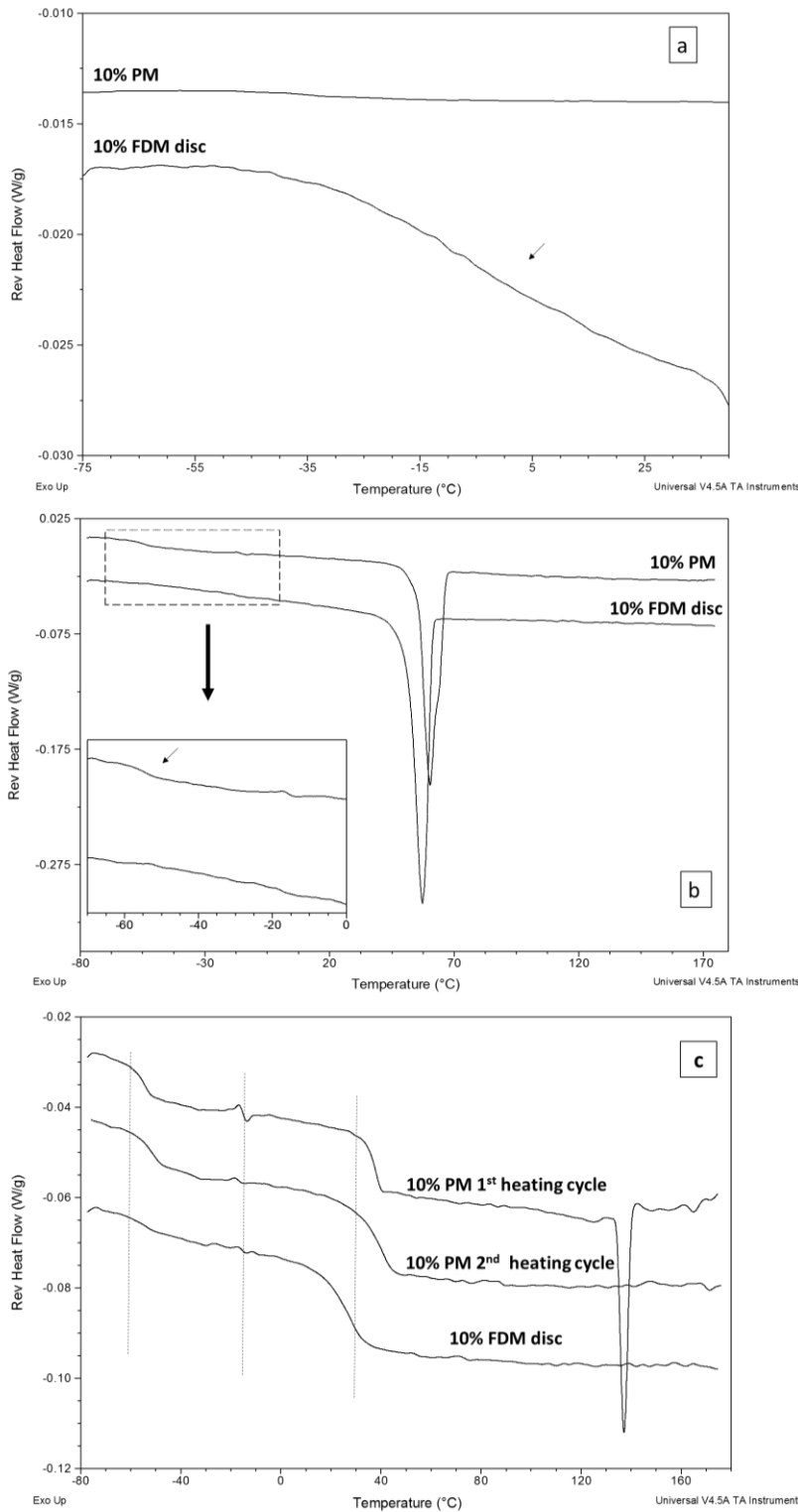


**Figure 6.** Partial ATR-FTIR spectra of the physical mixtures (PM) and felodipine loaded FDM printed discs. The NH stretching peak of crystalline felodipine is highlighted with the dashed line.

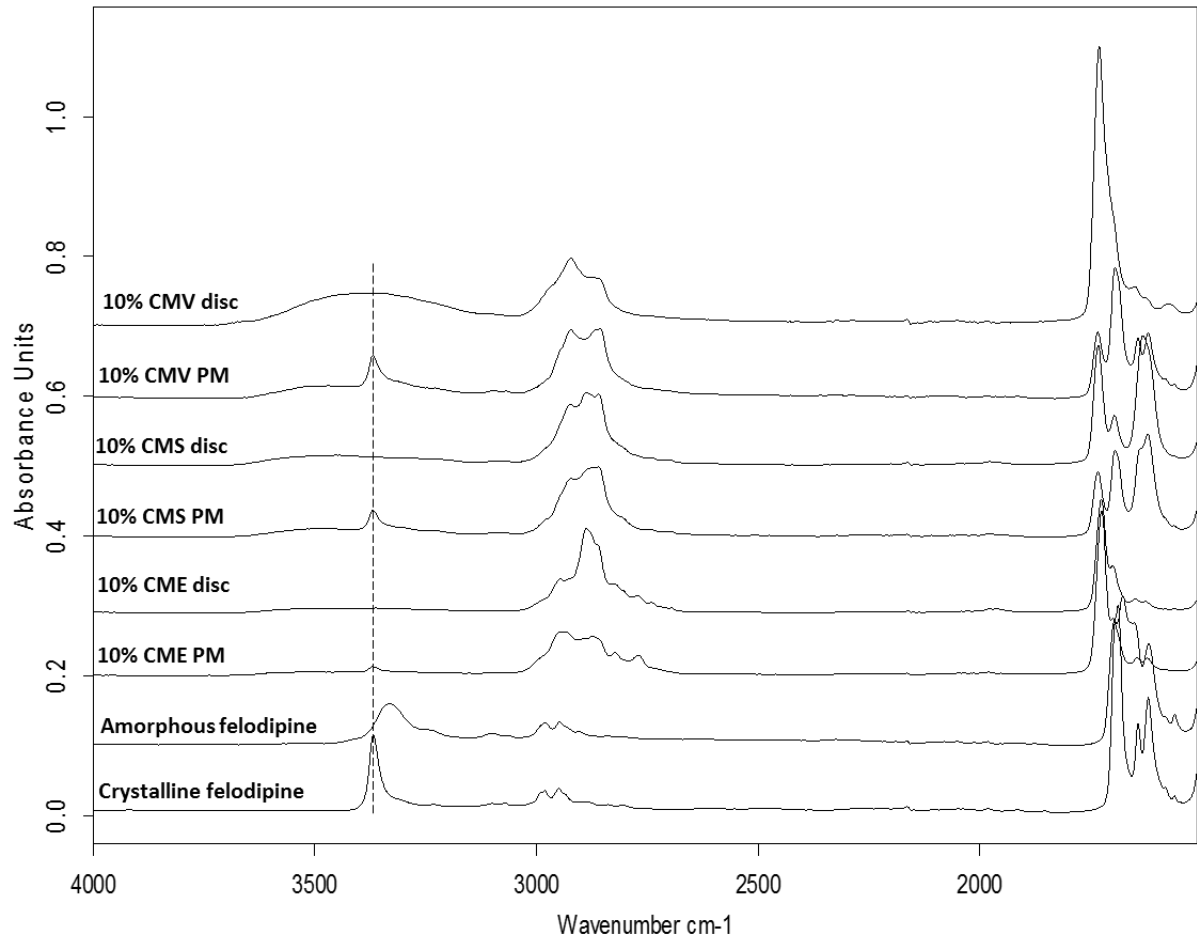


**Figure 7.** PXRD Diffraction patterns of (a) raw materials and (b) physical mixtures and 10% w/w felodipine loaded FDM printed CME, CMS and CMV discs.

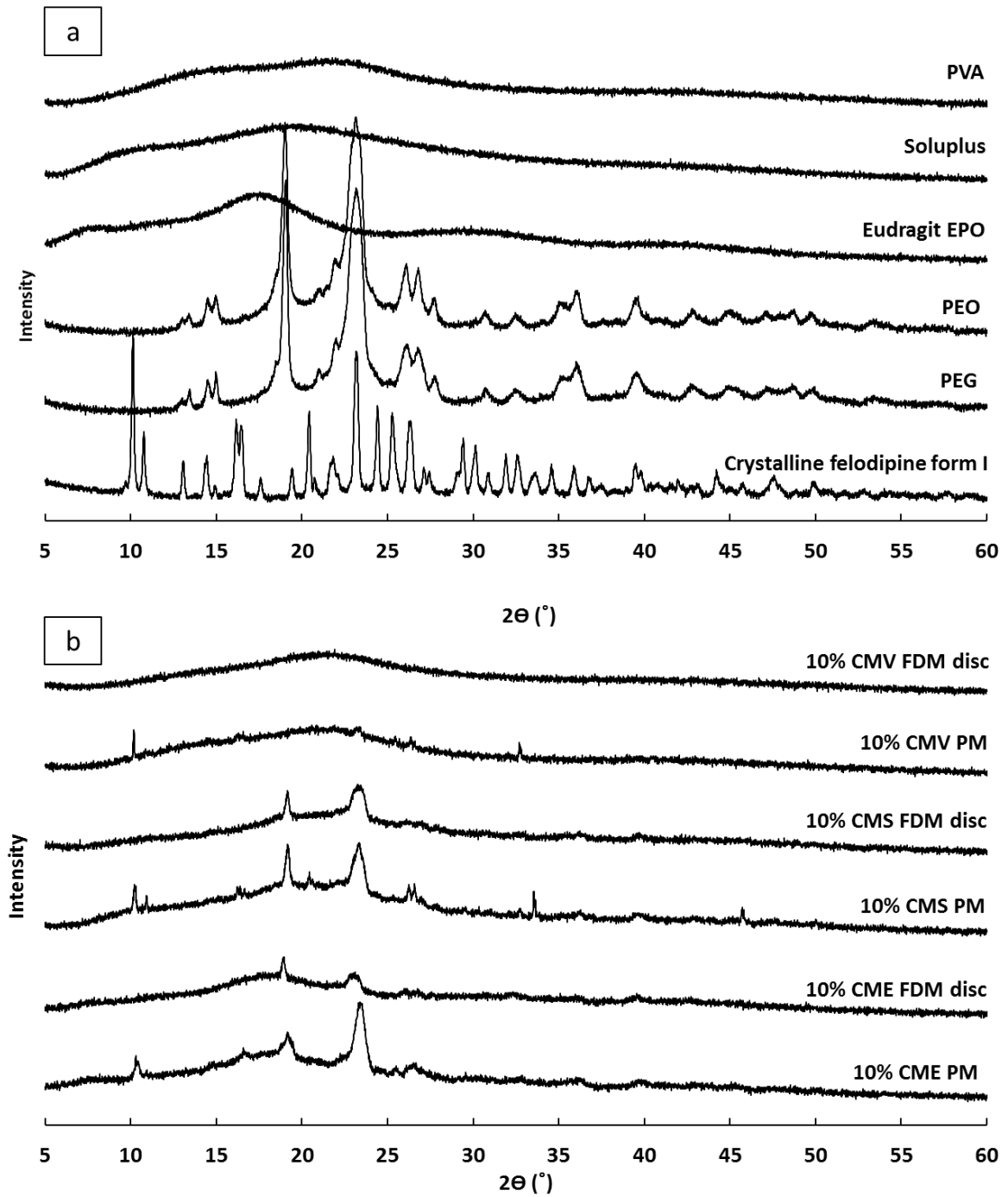


**Figure 8.** Felodipine release profile of FDM 3D printed discs using a) pH 1.2 HCl (simulated gastric fluid without enzyme) and b) pH 6.8 phosphate buffer saline (PBS).

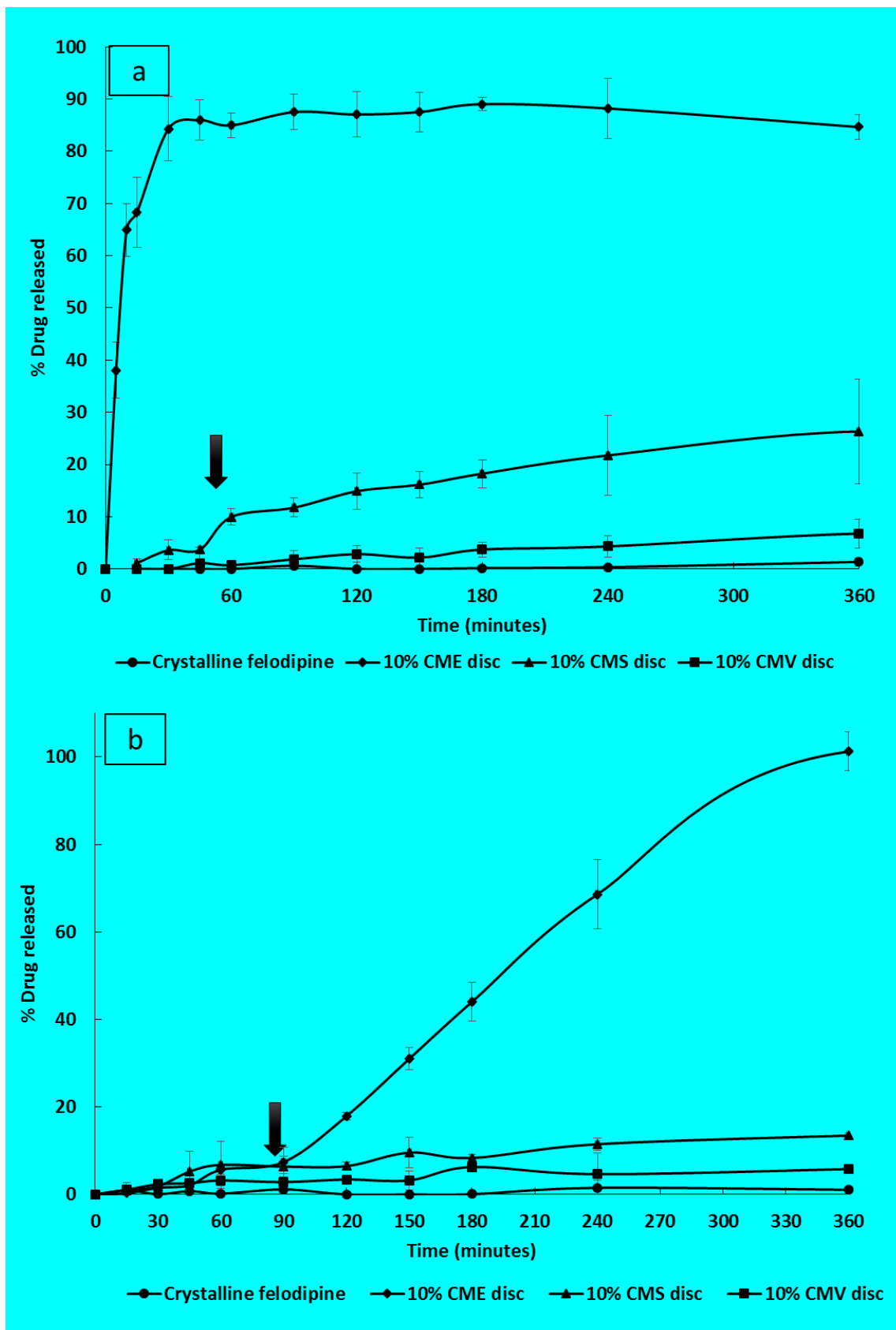


**Figure 9.** Visual appearances of felodipine loaded FDM printed CME discs during dissolution in pH 1.2 HCl and pH 6.8 PBS. The dash circles represent the diameters of freshly prepared dry CME discs.

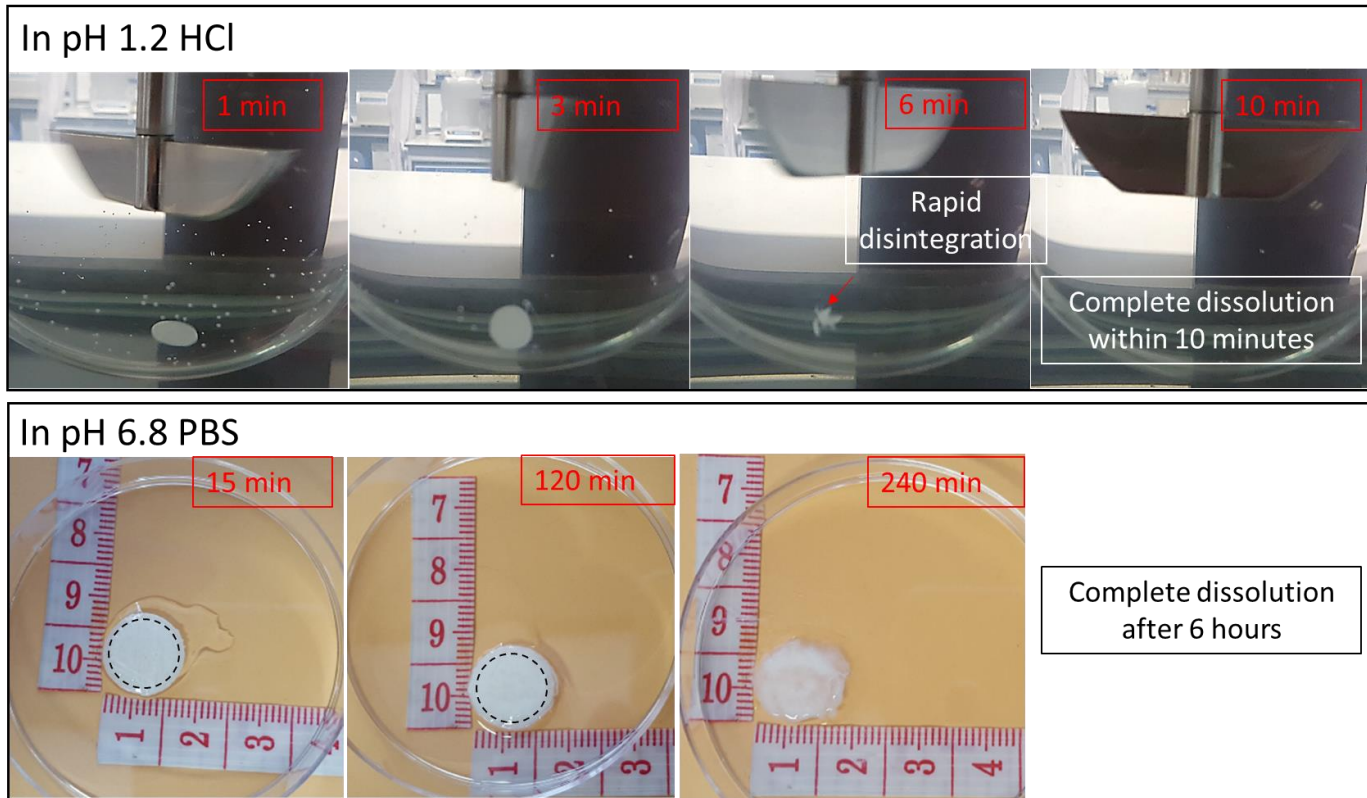


**Figure 10.** Visual appearances of the felodipine loaded FDM printed CMS discs during the dissolution tests in (a) pH 1.2 HCl and (b) pH 6.8 PBS; (c) the partial ATR-FTIR spectra and (d) DSC thermographs of the discs taken out of the media and dried after 6 hours dissolution. The dash circles in (a) and (b) represent the diameters of the dry and freshly prepared CMS discs. The dash lines in (c) highlight the felodipine related IR peaks and arrows highlight the changes of PEG/PEO related peaks labeled with \* before dissolution.

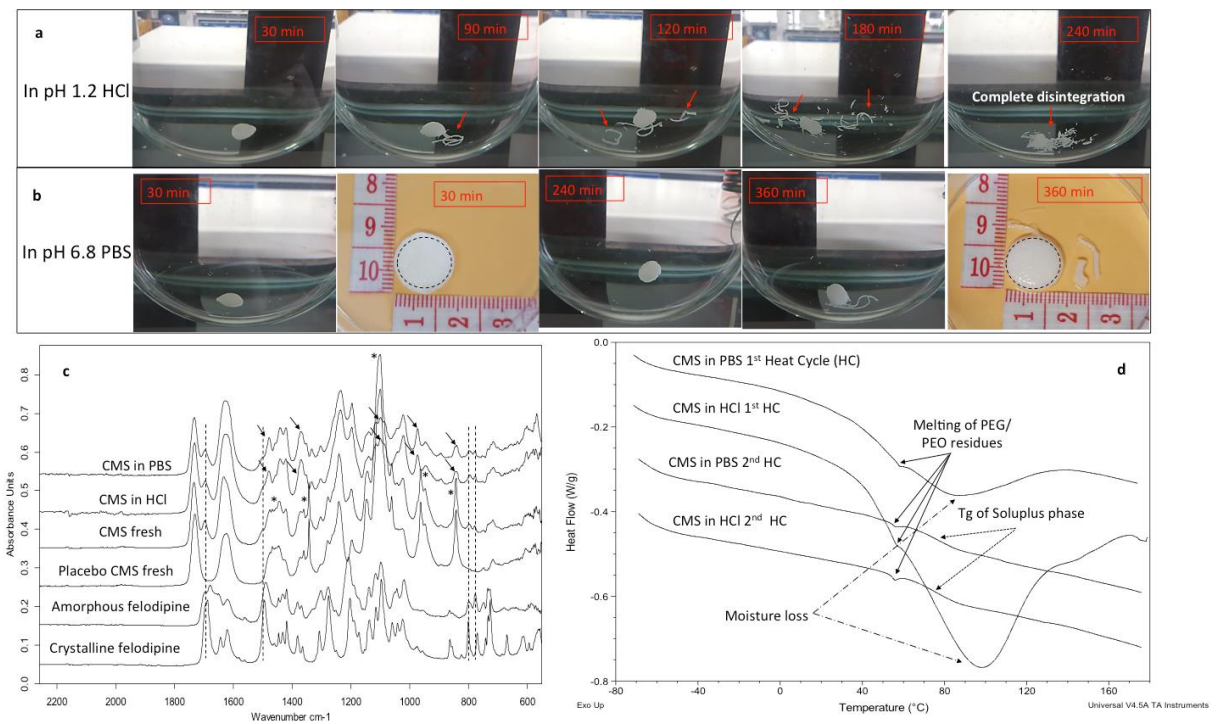


**Figure 11.** Visual appearances of the felodipine loaded FDM printed CMV discs during the dissolution tests in (a) pH 1.2 HCl and (b) pH 6.8 PBS; (c) the partial ATR-FTIR spectra and (d) DSC thermographs of the discs taken out of the media and dried after 6 hours dissolution. The dash circles in (a) and (b) represent the diameters of the dry and freshly prepared CMS discs.

